

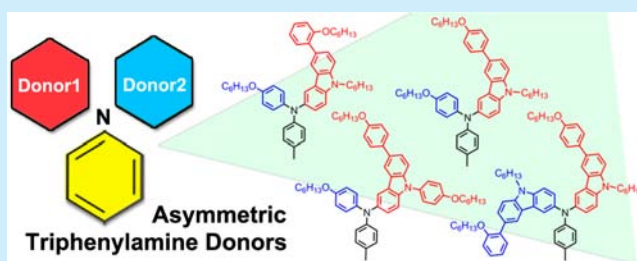
Novel Triphenylamine Donors with Carbazole Moieties for Organic Sensitizers toward Cobalt(II/III) Redox Mediators

Yulin Tan, Mao Liang,* Ziyi Lu, Yequan Zheng, Xinli Tong, Zhe Sun, and Song Xue*

Tianjin Key Laboratory of Organic Solar Cells and Photochemical Conversion, Department of Applied Chemistry, Tianjin University of Technology, Tianjin 300384, P.R. China

S Supporting Information

ABSTRACT: A series of D- π -A organic dyes, X72–75, containing novel triarylamine electron donors have been synthesized for dye-sensitized solar cells (DSCs). The superiority of the asymmetric design of the triphenylamine electron donor over the symmetrical triphenylamine when applied in organic dyes for cobalt cells has been observed. Using X72 with the cobalt(II/III) redox shuttle resulted in an overall power conversion efficiency (PCE) of 9.18%, outperforming the state-of-the-art dye C218 under the same conditions.



Dye-sensitized solar cells (DSCs) have attracted considerable attention since the initial work from Grätzel and co-workers.¹ Compared to inorganic silicon-based solar cells, low costs, and good efficiency are prominent features of DSCs.^{1b} In the past two decades, tremendous research efforts have been devoted to designing and synthesizing donor- π -acceptor (D- π -A) organic sensitizers,^{2–12} which currently reach more than 10% power-conversion efficiency (PCE).¹³ Recently, the combination of the cobalt(II/III) redox shuttles with high-absorption coefficient organic D- π -A dyes has brought forth a new opportunity to make a further breakthrough in efficiency. Fabrication of DSCs utilizing the [Co(bpy)₃]^{2+/3+} redox couple and SM315 exhibited a high photovoltage of 0.91 V and demonstrated a record 13% PCE at full sun illumination.¹⁴ Note that significant control of charge recombination and fine-tuning of the molecular energy level are still big challenges for the cobalt cells. To meet the requirements for effective light harvesting and control of the charge recombination to the cobalt(III) complexes, molecular engineering of the electron donor is a feasible strategy in developing organic sensitizers toward cobalt(II/III) redox mediators.

Triarylamines are well-known electron donors that are widely used in organic sensitizers, owing to their strong electron-donating ability and excellent hole-transporting ability.³ It is valuable to note that most triarylamines are symmetrical, namely, when two identical donors are substituted on an aniline (e.g., dihexyloxy-substituted triphenylamine or a bis-dimethyl-fluorenylamino moiety).³ Our strategy for obtaining highly efficient organic dyes toward the cobalt(II/III) redox shuttles is focused on asymmetric triphenylamine donors. This delicate architecture provides an opportunity to fine-tune the steric properties and the molecular energy level of organic dyes through the introduction of two donor moieties with different functions. By this approach, new families of sensitizers with

interesting properties would be produced as a result of judiciously varying the terminal donors.

In this study, three carbazole moieties (9-hexyl-3-(2-(hexyloxy)phenyl)-9H-carbazole, **2-HPC**; 9-hexyl-3-(4-(hexyloxy)phenyl)-9H-carbazole, **4-HPC**; 3,9-bis(4-(hexyloxy)phenyl)-9H-carbazole, **BHPC**) were employed to construct four novel triarylamine electron donors, enabling modulation of the steric properties and the molecular energy level of organic dyes. The synthesized organic dyes (X72, X73, X74, and X75) are shown in Figure 1, with the synthetic methodology of the X72–74 being highlighted in Scheme 1.

Compounds **5a–c** were obtained by the Suzuki coupling reaction of **1a,b** with **2**, followed by reduction of the nitro group and subsequent reaction with 1-bromo-4-(hexyloxy)benzene. These compounds were allowed to react with an aryl bromide **6** to produce **7a–c**. Aldehydes **8a–c** were synthesized by a Vilsmeier–Haack reaction of **7a–c** with POCl₃ and DMF.

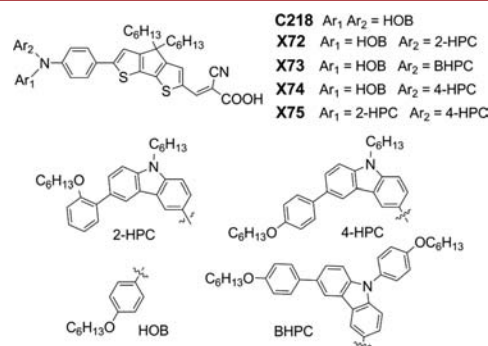
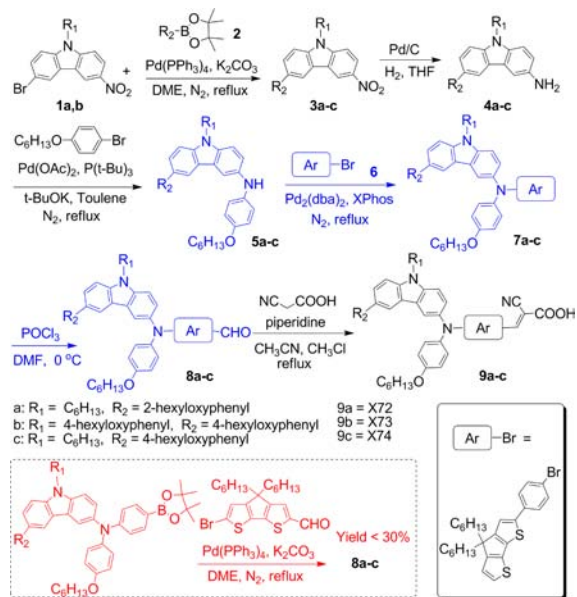


Figure 1. Structure of the synthesized dyes and C218.

Received: June 23, 2014

Published: July 24, 2014

Scheme 1. Schematic Diagram for the Synthesis of X72–74



Subsequently, the target dyes were obtained via Knoevenagel condensation reaction of the aldehydes **8a–c** with cyanoacetic acid in the presence of a catalytic amount of piperidine. Note that the yields of **8a–c** (red route) through the Suzuki reaction between a borate complex and 6-bromo-4,4-dihexyl-4H-cyclopenta[2,1-b:3,4-b']dithiophene-2-carbaldehyde are <30%. Furthermore, the products are very difficult to purify by column chromatography. In this work, the synthetic strategy incorporating a Buchwald–Hartwig reaction as the key step has been established for facile synthesis of **8a–c** (blue route). Compounds **5a–c** underwent a Buchwald–Hartwig amination, giving the desired **7a–c** with a 50–70% yield. A route that is different from the conventional way of triarylamine dyes synthesis. The synthetic route to X75 is shown in Scheme S1 in the Supporting Information (SI). The detail characterization data of the dyes are also provided in the SI.

UV–vis absorption spectra of dyes in dichloromethane are presented in Figure 2, and their corresponding data are

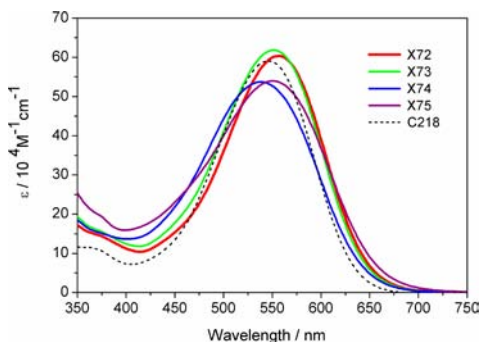


Figure 2. Absorption spectra of dyes in DCM.

summarized in Table 1. All dyes exhibit a single prominent band with the absorption maximum around ca. 540–560 nm. Among these sensitizers, the X72 dye with 2-HPC based triarylamine electron donor presents the longest maximum absorption wavelength of 556 nm, with a maximum molar absorption coefficient of 60 590 M^{−1} cm^{−1}. By comparison, constructing the X74 dye with 4-HPC leads to a blue-shifted

Table 1. Optical and Electrochemical Properties of the Dyes

dye	λ_{\max} (nm) ^a	ϵ (M ^{−1} cm ^{−1}) ^a	E_{0-0} (V) ^b	E_{D/D^+} (V) ^c	E_{D^*/D^+} (V) ^d
X72	556	60 590	2.01	0.86	−1.16
X73	550	61 850	2.03	0.88	−1.15
X74	539	53 760	2.04	0.85	−1.19
X75	553	54 170	2.04	0.80	−1.24
C218	546	59 000	2.06	0.90	−1.16

^aThe absorption spectra were measured in CH₂Cl₂ solutions. ^b E_{0-0} values were estimated from the intersections of normalized absorption and emission spectra ($\lambda_{\text{int}} E_{0-0} = 1240/\lambda_{\text{int}}$); see Figure S1. ^c E_{D/D^+} was recorded by cyclic voltammograms of the dye-loaded TiO₂ film. ^d E_{D^*/D^+} was calculated from $E_{D/D^+} - E_{0-0}$.

maximum absorption wavelength ($\lambda_{\max} = 539$ nm) and an attenuated maximum molar absorption coefficient ($\epsilon = 53 760$ M^{−1} cm^{−1}), indicating that the substituent alteration from 2-HPC to 4-HPC brings forth a weakened intramolecular charge transfer interactions. A 4-(hexyloxy)phenyl unit was introduced on the carbazole nitrogen atom for X73 leading to a bathochromic shift of 11 nm, as well as increasing the absorption intensity when compared to the X74, owing to the extended π -conjugation. On the other hand, upon incorporating two carbazole moieties, i.e. 2-HPC and 4-HPC, in triarylamine, X75 shows a distinct advantage over other dyes in the range of the absorption band. Note that all carbazole dyes exhibit a broader absorption compared with the UV–vis data recorded from the C218, which is beneficial to light-harvesting and thus short-circuit current enhancement.

We further carried out cyclic voltammogram measurements (Figure S2) to determine the accurate E_{D/D^+} values of these dye sensitized films (Table 1), by averaging the anodic and cathodic peak potentials. Generally, the carbazole based dyes have a lower first oxidation potential than that of the C218 dye, suggesting the feature of being electron-rich for 2-HPC, 4-HPC, and BHPC moieties. Note that the E_{D/D^+} of X75 (0.80 V) is much lower than those of X72–74 (0.85–0.88 V) as result of two carbazole donors being introduced, resulting in an attenuated driving force for the regeneration of the oxidized dye. It is obvious that the asymmetric design of triphenylamine donor can be used to fine-tune the organic dye HOMO level so as to achieve efficient dye regeneration and at the same time maximize the open circuit potential. The calculated excited-state potentials of these dyes (−1.15 to −1.24 V vs NHE) are placed sufficiently above the TiO₂ conduction band edge to ensure no energetic barriers for the electron injection.

Further insight into the molecular structure and frontier molecular orbitals of these dyes was performed via density functional calculations. An optimized geometrical configuration of the dyes can be found in Figure S3, and selected frontier orbitals of the dyes are shown in Figure S4. Examination of the HOMO and LUMO of X72–75 indicates that HOMO–LUMO excitation moves the electron distribution from the triarylamine donor to the cyanoacrylic acid moiety via a π -space group, allowing efficient charge separation and electron injection.

Owing to the poor solubility of X72–75 in the routine DSC dye bath solvents (e.g., *t*-BuOH and acetonitrile (MeCN)), a binary solvent of DCM and *t*-BuOH was our preliminary choice for the adsorption of dyes on a mesoporous titania film. However, this mixed solvent does not lead to satisfied photovoltaic performance (Table S1), owing to a low grafting density of dyes on titania (Figure S5). By contrast, use of a

ternary dye bath solvent, including MeCN with DCM and *t*-BuOH dramatically improved DSC device performance. Based on a mixed solvent of *t*-BuOH–MeCN–DCM (1.5:1.5:2 volume ratio), DSC devices were fabricated using the carbazole dyes to compare the influence of the electron donor variations on the photovoltaic parameters. The photocurrent density voltage curves (*J*–*V*) of the devices employing the Co-bpy electrolyte under AM 1.5 irradiation (100 mW cm^{−2}) were recorded, and the detailed photovoltaic parameters were compiled in Table 2. As Figure 3a presents, the short-circuit

Table 2. DSCs Performance Parameters of the Investigated Dyes

dye	J_{SC} (mA cm ^{−2})	V_{OC} (mV)	FF	PCE/%
X72	14.6	925	0.68	9.18
X73	13.5	937	0.67	8.47
X74	14.0	913	0.68	8.69
X75	13.8	901	0.67	8.33
C218	13.8	865	0.69	8.35

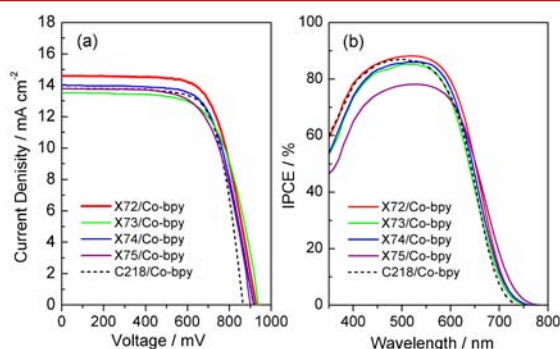


Figure 3. (a) *J*–*V* curves for DSCs based on the dyes under illumination of AM 1.5 G simulated sunlight (100 mW cm^{−2}). (b) IPCE spectra of the same DSCs.

photocurrent density (J_{SC}), open-circuit photovoltage (V_{OC}), and fill factor (FF) of the X74 cell are 14.0 mA cm^{−2}, 913 mV, and 0.68, respectively, affording a power conversion efficiency (PCE) of 8.69%. Furthermore, an improved J_{SC} of 14.6 mA cm^{−2} concomitant with an increased V_{OC} of 925 mV was achieved with the X72 dye, contributing to a higher PCE of 9.18%, indicative of the superiority of 2-HPC over 4-HPC when applied in triarylamine organic dyes. Despite the highest V_{OC} , the X73 cell exhibits a much lower PCE compared to the X72, primarily owing to the significantly attenuated photocurrents. It is noteworthy that, in comparison to the case of the C218 dye, the employment of the X72–74 brings forth evidently enhanced PCE, demonstrating the superiority of the asymmetric design of the triphenylamine electron donor over the symmetrical triphenylamine when applied in organic dyes for cobalt cells. One may argue that this is not true because X75 shows a comparable PCE of C218. Worthy of note, the HOMO level of X75 is significantly influenced by the two carbazole units rather than the 2-(hexyloxy)phenyl or 4-(hexyloxy)phenyl group; at the same time, the regeneration and recombination kinetics in cobalt cells are closely related to the HOMO level of the dyes. From this point of view, the triarylamine in X75 can be thought to be a symmetrical structure.

We further carried out the incident photon-to-collected electron conversion efficiency (IPCE) measurements of the cobalt cells. The IPCE spectra of the devices made with these

dyes closely follow the absorption spectra of the dye-grafted translucent titania films in contact with the Co-bpy electrolyte for cell fabrication (Figure S6). As shown in Figure 3b, the X72 cell exhibits a broad plateau with a higher IPCE summit compared to the X73 and X74 counterparts, which contributes to the higher J_{SC} of X72. It is valuable to note that the X75 confers a lower IPCE from 350 to 600 nm as compared to those obtained with X72–74, a result that can mainly be attributed to the small driving force for regeneration (reasons have been provided in pp S67–68 in SI). Furthermore, for Co-bpy cells, the driving force for regeneration of X75 is only 0.24 eV, much lower than those of X72–74. Assuming that an energy gap of 0.4 eV is necessary for efficient regeneration,¹⁵ this may induce inferior regeneration efficiency. Nevertheless, this loss in IPCE is compensated by a gain in longer wavelength, resulting in a J_{SC} value as high as that for X73. By contrast, the IPCE response of C218 is relatively narrower than other dyes, despite its high response in this spectral region.

To examine the energetic and dynamic origins of the observed V_{OC} difference, we performed charge-extraction and transient photovoltage decay measurements. As presented in Figure 4a, cells made with X72 and C218 display a similar

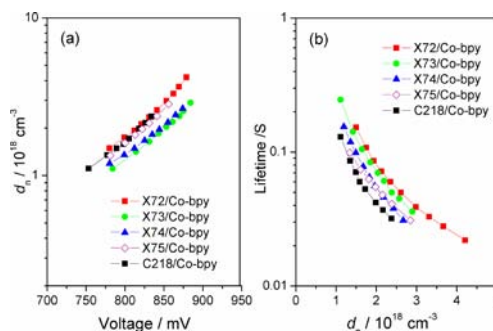


Figure 4. (a) Charge density at open circuit and (b) electron lifetime as a function of charge density for DSCs.

extracted electron density (d_n) at the same potential bias, indicative of a fixed conduction-band (CB) edge of titania with respect to the electrolyte Fermi level. The dye alteration from X72 to X74 caused the TiO₂ bands to be shifted upward by about 30 mV. Possible causes are thought to be correlated with the dye coverage and the interaction between TiO₂ and TBP.¹⁶ However, the relatively higher conduction band edge of the X74 cell does not lead to an improved V_{OC} due to the attenuated electron lifetime. As the photocurrent decay measurements indicate (Figure 4b), for these asymmetric triphenylamine dyes, the 2-HPC donor leads to the longest lifetimes, whereas the 4-HPC and BHPC donors shorten the lifetimes. Furthermore, X75 featuring a bulky triphenylamine donor exhibits a shortened lifetime, a result that is thought to be correlated with the small driving force for the regeneration of the oxidized dye, because an inefficient regeneration of dye cations also promotes the interfacial recombination of titania electrons with electron-accepting species in an electrolyte and/or dye cations. For C218, a shorter electron lifetime has been measured compared to devices incorporating X72–75, giving a clear clue regarding its smaller photovoltage.

In summary, we have synthesized four D– π –A organic sensitizers with novel triarylamine donors for DSC applications through a facile method where the π -conjugated bridge was introduced into dyes via a Buchwald–Hartwig reaction. Not

only was the electron-donating ability stronger in the absence of carbazole moieties but also the unfavorable recombination between the electrolyte and the TiO₂ surface was reduced as well. The device based on the sensitizer X72 gave an overall conversion of 9.18%, which is higher than that of the state-of-the-art dye C218 under the same conditions. This work provides a new paradigm for developing new D- π -A organic sensitizers for DSCs employing the cobalt redox couples.

■ ASSOCIATED CONTENT

Supporting Information

Experimental details, characterization data for all new compounds, details of the DSC fabrication, cyclic voltammogram, emission spectra, molecular orbitals, and cell characterizations. This material is available free of charge via the Internet at <http://pubs.acs.org>.

■ AUTHOR INFORMATION

Corresponding Authors

*E-mail: liangmao717@126.com.

*E-mail: xuesong@ustc.edu.cn.

Notes

The authors declare no competing financial interest.

■ ACKNOWLEDGMENTS

We gratefully acknowledge the financial support from the National 973 Program (No. 2011CBA00702), the National Science Foundation of China (No. 21373007, 21376179), and the Tianjin Natural Science Foundation (13JCZDJC32400, 14JCYBJC21400).

■ REFERENCES

- (1) O'Regan, B.; Grätzel, M. *Nature* **1991**, 353, 737–740.
- (b) Hagfeldt, A.; Boschloo, G.; Sun, L.; Kloo, L.; Pettersson, H. *Chem. Rev.* **2010**, 110, 6595–6663.
- (2) Yen, Y.-S.; Chou, H.-H.; Chen, Y.-C.; Hsu, C.-Y.; Lin, J. T. *J. Mater. Chem.* **2012**, 22, 8734–8747.
- (3) Liang, M.; Chen, J. *Chem. Soc. Rev.* **2013**, 42, 3453–3488.
- (4) Cai, L.; Moehl, T.; Moon, S.-J.; Decoppet, J.-D.; Humphry-Baker, R.; Xue, Z.; Liu, B.; Zakeeruddin, S. M.; Grätzel, M. *Org. Lett.* **2014**, 16, 106–109.
- (5) Lim, B.; Margulis, G. Y.; Yum, J.-H.; Unger, E. L.; Hardin, B. E.; Grätzel, M.; McGehee, M. D.; Sellinger, A. *Org. Lett.* **2013**, 15, 784–787.
- (6) (a) Gao, P.; Tsao, H. N.; Grätzel, M.; Nazeeruddin, M. K. *Org. Lett.* **2012**, 14, 4330–4333. (b) Gao, P.; Kim, Y. J.; Yum, J.-H.; Holcombe, T. W.; Nazeeruddin, M. K.; Grätzel, M. *J. Mater. Chem. A* **2013**, 1, 5535–5544.
- (7) (a) Velusamy, M.; Thomas, K. R. J.; Lin, J. T.; Hsu, Y.-C.; Ho, K.-C. *Org. Lett.* **2005**, 7, 1899–1902. (b) Chaurasia, S.; Hung, W.-I.; Chou, H.-H.; Lin, J. T. *Org. Lett.* **2014**, 16, 3052–3055.
- (8) (a) Wang, Z.; Liang, M.; Wang, H.; Wang, P.; Cheng, F.; Sun, Z.; Xue, S. *ChemSusChem* **2014**, 7, 795–803. (b) Li, G.; Liang, M.; Wang, H.; Sun, Z.; Wang, L.; Wang, Z.; Xue, S. *Chem. Mater.* **2013**, 25, 1713–1722. (c) Sun, Z.; Zhang, R.-K.; Xie, H.-H.; Wang, H.; Liang, M.; Xue, S. *J. Phys. Chem. C* **2013**, 117, 4364–4373. (d) Wang, Z.; Wang, H.; Liang, M.; Tan, Y.; Cheng, F.; Sun, Z.; Xue, S. *ACS Appl. Mater. Interfaces* **2014**, 6, 5768–5778.
- (9) Zhu, W.; Wu, Y.; Wang, S.; Li, W.; Li, X.; Chen, J.; Wang, Z.-S.; Tian, H. *Adv. Funct. Mater.* **2011**, 21, 756–763.
- (10) Koumura, N.; Wang, Z.-S.; Mori, S.; Miyashita, M.; Suzuki, E.; Hara, K. *J. Am. Chem. Soc.* **2006**, 128, 14256–14257.

(11) Murakami, T. N.; Koumura, N.; Uchiyama, T.; Uemura, Y.; Obuchi, K.; Masaki, N.; Kimura, M.; Mori, S. *J. Mater. Chem. A* **2013**, 1, 792–798.

(12) Liu, B.; Wang, B.; Wang, R.; Gao, L.; Huo, S.; Liu, Q.; Li, X.; Zhu, W. *J. Mater. Chem. A* **2014**, 2, 804–812.

(13) (a) Cao, Y.; Cai, N.; Wang, Y.; Li, R.; Yuan, Y.; Wang, P. *Phys. Chem. Chem. Phys.* **2012**, 14, 8282–8286. (b) Tsao, H. N.; Burschka, J.; Yi, C.; Kessler, F.; Nazeeruddin, M. K.; Grätzel, M. *Energy Environ. Sci.* **2011**, 4, 4921–4924. (c) Yella, A.; Humphry-Baker, R.; Curchod, B. F. E.; Astani, N. A.; Teuscher, J.; Polander, L. E.; Mathew, S.; Moser, J.-E.; Tavernelli, I.; Rothlisberger, U.; Grätzel, M.; Nazeeruddin, M. K.; Frey, J. *Chem. Mater.* **2013**, 25, 2733–2739. (d) Yang, J.; Ganesan, P.; Teuscher, J.; Moehl, T.; Kim, Y. J.; Yi, C.; Comte, P.; Pei, K.; Holcombe, T. W.; Nazeeruddin, M. K.; Hua, J.; Zakeeruddin, S. M.; Tian, H.; Grätzel, M. *J. Am. Chem. Soc.* **2014**, 136, 5722–5730.

(14) Mathew, S.; Yella, A.; Gao, P.; Humphry-Baker, R.; Curchod, B. F. E.; Ashari-Astani, N.; Tavernelli, I.; Rothlisberger, U.; Nazeeruddin, M. K.; Grätzel, M. *Nat. Chem.* **2014**, 6, 242–247.

(15) Feldt, S. M.; Lohse, P. W.; Kessler, F.; Nazeeruddin, M. K.; Grätzel, M.; Boschloo, G.; Hagfeldt, A. *Phys. Chem. Chem. Phys.* **2013**, 15, 7087–7097.

(16) Zhang, J.; Yao, Z.; Cai, Y.; Yang, L.; Xu, M.; Li, R.; Zhang, M.; Dong, X.; Wang, P. *Energy Environ. Sci.* **2013**, 6, 1604–1614.